Hybrid Cyclotriphosphazene-Phenothiazine-Hydrozone Material with Tunable Yellow-Green Emitting Properties

Dinesh Kumar Chelike[1,2], Senthil A. Gurusamy Thangavelu[2*], Ananthanarayanan Krishnamoorthy[2*]

[1]Department of Chemistry, Rungta College of Engineering & Technology, Bhilai-490024 Chhattisgarh India

[2]Research Institute, Department of Chemistry, SRM Institute of Science and Technology, Kattankulathur, Chennai 603203, Tamil Nadu, India

Abstract

A novel luminescent hybrid inorganic-organic molecular assembly was synthesised by the condensation of hexakis cyclotriphosphazene hydrazide (CTP-Hyd) with six units of 10-octyl-10H-phenothiazine-3-carbaldehyde (R-PTZ-CHO). In particular, synthesis of new precursor from inorganic heterocycle, CTP-Hyd has been developed to append the PTZ units on the periphery of thermally stable CTP ring via condensation for the first time. The luminescent hybrid prepared by convergent approach was well characterized at each step using plethora of techniques like FT-IR, multi-nuclear NMR including ^{1}H, ^{13}C and ^{31}P spectra as well as HR MS/MALDI-TOF data. Further, the photophysical properties were investigated by UV-*vis*, photoluminescence and time resolved photoluminescence spectroscopy. The synthesised molecule shows extraordinary solvent compatibility and shows tunable emission in the yellow-green region. Relatively a large stokes shift of 82 nm was observed with varying solvent polarity. Thermal and electrochemical properties of key substrates and products were studied using thermal gravimetric analysis (TGA) and cyclic voltammetry.

Keywords: cyclotriphosphazene hydrazide, phenothiazine aldehyde, hydrazone Schiff base, hybrid organic-inorganic, photophysical studies, solvent effect

I. INTRODUCTION

In recent times, hybrid inorganic-organic framework materials were developed using assembly of multi-chromophore moieties on inorganic scaffold in order to explore with various applications including the areas of photophysics and photochemisty [1-5]. In these hybrid systems, merits of organic units use to be enhanced in terms of stability, thermal and mechanical as well as physicochemical properties [6-8]. To substantiate the mutual role of organic and inorganic components in hybrid structure, choice of potential synthons and suitable synthetic route has to be established efficiently [9,10]. As an organic counterpart of hybrid structure, molecules such as rhodamine, fluorescein, phthalocyanine, fluorine, anthracene, naphthol, dansyl, phenanthroline, bianthracene and pyrene were explored in previous reports [5,11-14]. Amidst various organic molecules, phenothiazine (PTZ) was chosen in this present study due to its unique property of bowl shape non-planar electron donating heteroaromatic structure fused via sulphur and nitrogen atoms with a tendency to extend conjugation. Pristine phenothiazine (PTZ) exhibits strong fluorescence in solution and generation of donor-acceptor (D-A) properties in the structure is achieved by straightforward chemical method, for example N-alkylation and formylation affording R-PTZ-CHO (R = $-CH_3$, $-C_2H_5$, $-C_4H_{10}$ and $-C_6H_{14}$) [15]. R-PTZ-CHO was subjected to condense with tris(2-aminoethyl)amine to form Schiff bases and their photophysical properties was studied and phenothiazine-derived Schiff base was also encapsulated with silica cross-linked micellar nanoparticles units for the selective detection of Fe^{3+} ion in blood, based on fluorescence quenching [16,17]. Indeed, the desired properties of such organic units tend to be exploited efficiently while incorporated or functionalized on support of inorganic moiety [12,18].

Inorganic heterocycle, cyclotriphosphazene (CTP) was renowned for its planar ring and robust framework of cyclic structure, $[-N=PCl_2-]_3$ with six reactive chlorine to undergo nucleophilic substitution with variety of organic reagents (-OH, $-NH_2$, -SH etc.) [19,20]. The chemistry developed with ring type small molecule like CTP can be certainly translated to extend with polymeric substrate, polyphosphazene $[-N=PCl_2-]_n$, since CTP can be readily converted into $[-N=PCl_2-]_n$ via ring opening polymerization [21]. In the literature we found few examples of hybrid assemblies based on the reaction of organic unit tethered with amine/hydroxyl groups on inorganic heterocycle, CTP, those hybrid products exhibited unique photophysical and electrochemical properties [5,11-14]. In terms of reactivity of hydroxyl group reagents, CTP was appended via aryloxy link with versatile organic molecules such as tetraaryl pyrazole, oxy-naphthylchalcone, hexa boron-dipyrromethene, fulleropyrrolidine-pyridine, porphyrin, adamantane and imidazole/benzimidazole [22-27]. Similarly, CTP was also subjected to react via amine group of organic molecules such as phenanthroline, 9-aminophenalenimine, 1,9-disubstituted-phenalene and naphthalene [28-31]. Though there are few examples of amine substituted organic molecules on the CTP ring, hydrazide substituted precursor of phosphorus which is used to undergo condensation with aldehyde tethered organic molecules to form hydrazone Schiff bases are relatively scarce and such products were reported by Majoral and co-workers [32]. These reports encouraged us to synthesize a new type of hexakis hydrazide cyclotriphosphazene [N_3P_3(-NH-NH_2)$_6$, CTP-Hyd] as an inorganic counterpart to form an unprecedented assembly of six PTZ units via condensation reaction with R-PTZ-CHO (R=C_8H_{17}-) to form hexakis hydrazone Schiff base of PTZ on periphery of CTP for the first time.

The pioneering reports on chemistry of phosphorus hydrazide and its synthesis has to be described prior to the illustration of the newly developed CTP-Hyd as an essential scaffold in the present work. Both CTP and acyclic phosphorus (V) chloride were used to afford phosphorus (V) hydrazides as synthon for the facile conversion into hydrazone Schiff bases units of dendrimers, macrocycles and multisite ligands for various applications [12,32]. Majoral JP coworkers have reported reaction of N-methylhydrazine ($NMeHNH_2$) with $RP(X)Cl_2$ (R = Ph, NMe_2; X = O, S) to form phosphorus dihydrazides, $RP(X)(NMeNH_2)_2$ and extended on CTP to afford (N_3P_3(-N(Me)-NH_2)$_6$ [33]. Such phosphorus (V) hydrazide was obtained with terminal amine group after regiospecific substitution at the centre of –NH(Me) due to the inductive effect of methyl group, one of us explored the above precursors to form multi-ferrocene assembly, tetranuclear copper complex and macrocycles [34-36]. Despite the hydrazone link reported in previous literature, hydrazone formed from CTP-Hyd would be distinct, since the primary amine group adjacent to secondary amine substituted at phosphorus centre involved in Schiff base/hydrazone bond formation between inorganic and organic moieties. To our knowledge, PTZ-CTP is an unprecedented example, synthesized as an assembly of six PTZ units on CTP core by simple condensation between CTP-Hyd and R-PTZ-CHO under mild reaction condition. In our recent report, another hydrazide formed by reaction of hydrazine hydrate ($NH_2.NH_2.H_2O$) with ester group of methyl salicylate (X-COOMe, R = OHC_6H_4-) to afford the hydrazide (R-CO-NH-NH_2) and chosen to condense with pentakis salicyloxy CTP in order to tether on surface of Fe_3O_4 NPs towards cytotoxicity studies [37]. Certainly, the non-trivial hydrazone framework in assembly of chromophoric PTZ units on CTP can be anticipated to demonstrate characteristic photophysical and physicochemical properties, since the association of the above organic and inorganic counterpart in hybrid structure is being attempted for the first time.

II METHODOLOGY

Synthesis of CTP-PTZ hybrid inorganic-organic substrate was achieved by the convergent approach as illustrated in **Scheme 1**. The robust and reactive inorganic ring structure of CTP with six reactive chlorine atoms has been chosen to support the array of organic moiety, six units of phenothiazine (PTZ) at the periphery of three P (V) centres without steric hindrance. In the case of phenothiazine unit, N-alkylation followed by formylation step was performed using suitable reagents. 1-bromooctane was taken as a reagent and reacted with PTZ in the presence of NaOH using DMSO as solvent at ambient condition to yield octyl substituted PTZ [38]. Also, the addition of POCl3 into DMF under ice-acetone cold bath followed by reaction with octyl substituted PTZ in DCE medium at reflux condition occurred to introduce an electron withdrawing aldehyde group at 3-position of aromatic ring to yield a donor-acceptor (D-A) type compound [15].

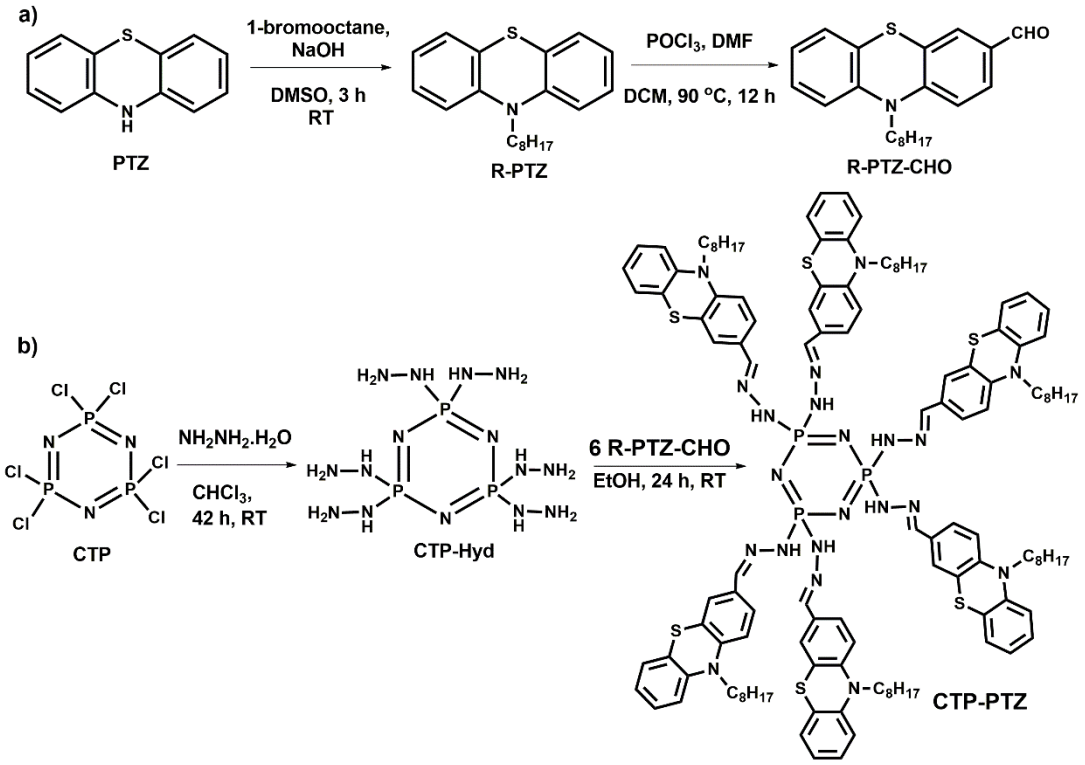

Scheme 1. **Synthesis of hybrid molecule a) synthesis of organic component, R-PTZ-CHO and b) synthesis of inorganic component, CTP-Hyd as well as the final product, CTP-PTZ.**

In another facet, hexakis hydrazide CTP (N_3P_3-(NH-NH_2)$_6$, CTP-Hyd) was obtained by the replacement of all chlorine atoms readily by nucleophilic substitution reaction using excessive hydrazine hydrate in $CHCl_3$ medium upon elimination of hydrazine hydrate hydrochloride under ambient condition. To synthesise the final hybrid product, CTP-PTZ, PTZ unit tethered with one aldehyde group (R-PTZ-CHO) and CTP substrate containing six terminal amine groups (CTP-Hyd) were allowed to undergo simple and feasible condensation in ethanol medium at ambient condition by elimination of water molecule as shown in **Scheme 1.** Generally, imine bond in Schiff base of hydrazone is commonly seen but the hybrid assembly of PTZ on CTP scaffold reported herein is an unprecedented example.

2.1 Synthesis of cyclotriphosphazene hydrazide (CTP-Hyd)

CTP-Hyd was synthesised by the modified procedure reported using the reagent, $NMeHNH_2$. [34]. CTP (0.500 g, 1.43 mmol) was weighed in RB flask (50 mL) and stirred for 10 min. in dry chloroform (30 ml) to dissolve at ambient temperature. After dissolution of CTP, RB flask was dipped into ice bath at 0 ^{o}C to cool down the solution before drop wise addition of hydrazine hydrate (99 %, 0.863 g, 17.26 mmol) for 30 min under vigorous stirring. After 1 h, ice bath was removed from the reaction mixture and allowed to stir at ambient temperature for 42 h. The white precipitate of hydrazine hydrochloride was filtered off and the reaction mixture was concentrated under vacuum to obtain viscous liquid. To obtain the pure white solid, viscous liquid was triturated with hexane (4×5 mL) under cold condition and discarded to remove impurities and evacuated under vacuum. Yield: 0.360 g, 77.6 % M.P. 200 ^{o}C ^{31}P {^{1}H} NMR (DMSO-d_6, 400 MHz): 8.64 ppm, FT-IR (cm^{-1}): 3332 (-$NH_{2\ str.}$), 1592 (-N-$H_{ben,}$), 1157 (-P-N), 1089 (-N-N-), 730 (P-N) and MALDI-TOF: 322.10 [M+1]$^{+}$ ion peak.

2.2 Synthesis of 10-octyl-10H-phenothiazine-3-carbaldehyde (R-PTZ-CHO)

R-PTZ-CHO was synthesised by adapting the synthetic protocol reported earlier [15]. In a clean and dry RB flask (100 mL), DMF (3.36 mL, 43.34 mmol) was added and kept in ice-acetone cold bath before addition of $POCl_3$ (4.05 mL, 43.34 mmol) taken in syringe for 10 min. After 30 min., the reaction mixture was removed from ice bath and stirred at ambient temperature for 1 h. In another RB flask (100 mL), R-PTZ (4.5 g, 14.45 mmol) was charged to dissolve in dry DCE (45 mL) and degassed by nitrogen gas and transferred to a dropping funnel to add into the above mixture while kept at ice-acetone cold bath for 30 min. After 30 min. the reaction mixture was stirred at ambient temperature for 1 h and subjected to reflux at 90 ^{o}C for 4h. After cooled down to ambient temperature, reaction mixture was poured into ice cubes in beaker (500 ml) under stirring. DCM (4 X 250 mL) was used to extract the product from the reaction mixture before discarding aqueous layer. The extract of organic layer was washed with brine solution (2 X 100 mL) and dried with anhydrous Na_2SO_4.

After evaporation of solvent, yellow viscous liquid product was isolated from silica gel column using the eluent, hexane- ethyl acetate (19:1). Yield 3.6 g 73.1 %.
^{1}H NMR (Chloroform-*d*, 500 MHz) δ ppm: 0.86 (t, *J*=6.87 Hz, 3 H) 1.21 - 1.35 (m, 8 H) 1.39 - 1.48 (m, 2 H) 1.81 (m, 2 H) 3.88 (t, *J*=7.25 Hz, 2 H) 6.88 (t, *J*=8.39 Hz, 2 H) 6.94 - 6.99 (m, 1 H) 7.08 - 7.12 (m, 1 H) 7.13 - 7.19 (m, 1 H) 7.57 - 7.60 (m, 1 H) 7.63 (dd, *J*=8.39, 1.72 Hz, 1 H) 9.79 (s, 1 H). ^{13}C NMR (125 MHz, Chloroform-*d*)□□ ppm: 189.90, 150.61, 143.32, 130.94, 130.11, 128.19, 127.41, 124.86, 123.65, 123.51, 115.93, 114.72, 47.93, 32.65, 31.76, 29.12, 26.77, 22.67, 14.12. HR-MS: 340.170 [M^{+}] ion peak.

2.3 Synthesis of hybrid inorganic-organic hydrazone Schiff base, CTP-PTZ

The suspension of CTP-Hyd (0.100 mg, 0.312 mmol) in ethanol (15 mL) was stirred for 30 min., the solution of R-PTZ-CHO (0.687 g, 2.03 mmol) in ethanol (10 mL) was added drop wise into the above reaction at ambient temperature to stir for 24 h. After completed the reaction, orange solid compound was filtered and apply high vacuum to obtain dry compound. Yield: 0.660 mg, 94.5 % ^{1}H NMR (500 MHz, Chloroform-*d*) δ ppm: 0.87 (t, *J*=6.87 Hz, 18 H) 1.23 - 1.35 (m, 48 H) 1.43 (m, 12 H) 1.78 - 1.84 (m, 12 H) 3.86 (t, *J*=7.25 Hz, 12 H) 6.83 - 6.89 (m, 12 H) 6.91 - 6.96 (m, 6 H) 7.10 - 7.17 (m, 12 H) 7.54 - 7.61 (m, 12 H) 8.52 (s, 6 H). ^{13}C NMR (125 MHz, Chloroform-*d*) δ ppm: 160.76, 148.05, 144.40, 128.99, 128.50, 127.71, 127.58, 125.24, 124.29, 123.17, 115.83, 115.31, 47.98, 31.97 29.42, 27.11, 27.01, 22.86, 14.35. FT-IR (cm^{-1}) 2919 (m, -C-$H_{str.}$), 1608 (m, C=N), 1461 (s, C=C), 1217 (m, C-N), 1138 (s, -P=N), 741 (s, P-N), MALDI-TOF: 2245 [M^{+}] ion peak.

III RESULTS AND DISCUSSION

3.1 FT-IR data

FT-IR spectroscopy was used to characterise the final hybrid molecule, which was synthesised using a feasible procedure, as well as both types of important precursors, CTP-Hyd and R-PTZ-CHO. The results are displayed in **Figure 1**. The data in **Figure 1a** was used to determine the planar structure of CTP; the signal at 1179 cm^{-1} reflected the P-N-P degenerate ring stretching frequency, while the forbidden symmetric stretching frequency was seen at 875 cm^{-1} and there were also additional signals at 593 and 524 cm^{-1} [39]. According to **Figure 1b**, CTP-Hyd exhibits overlapping signals for N-H stretching at 3332 cm-1 and N-H bending at 1592 cm^{-1} when six terminal primary amines and corresponding secondary amines are linked to P (V) centres [34]. Additionally, shifted P-N stretching at 1157 cm^{-1}, the vibrational frequency corresponding to the hydrazide's -N-N bond at 1089 cm^{-1}, and a few signals between 860 and 520 cm^{-1} corroborated the existence of the CTP core ring. **Figure 1c** illustrates the FT-IR spectrum of R-PTZ-CHO. The octyl group was detected by the stretching frequencies of the -CH_3 and -CH_2-groups around 2960 and 2860 cm^{-1}, as well as the bending vibrations of the same groups at 1460 and 1440 cm^{-1}. Additionally, the carbonyl signal for the conjugated aldehyde was found at 1685 cm^{-1} along with the stretching frequency of -N-CH2 at 1456 cm^{-1} and the rocking frequency of long alkyl chains at 722 cm^{-1}. The spectrum obtained for the assembly of CTP-PTZ is given in **Figure 1d**, and it can be observed that the signal at 1608 cm^{-1} appears due to the production of an imine (-C=N-) bond, while the signal from the terminal amine group vanishes between 3332 and 1592 cm^{-1} [34]. The remaining signals between 1470 and 520 cm-1 corroborated the vibrational frequencies with regard to the P-N framework of the CTP ring and the six units of PTZ units [39].

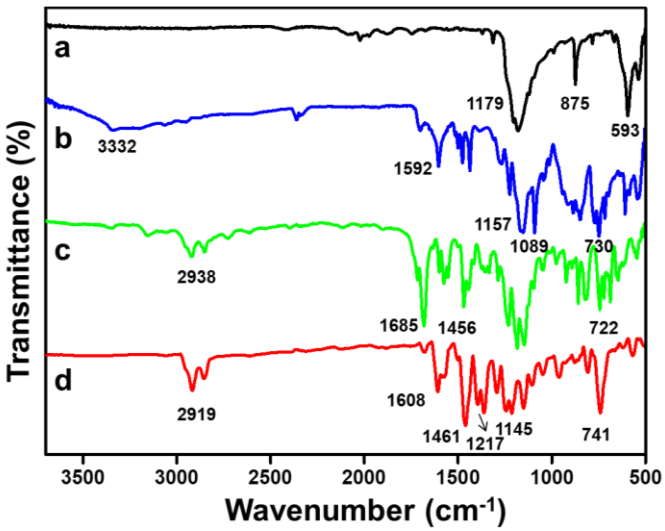

Figure 1. FT-IR data of synthesised compounds a) CTP, b) CTP-Hyd, c) R-PTZ-CHO and d) CTP-PTZ.

3.2 ^{1}H, ^{13}C NMR and HRMS data of hybrid molecule CTP-PTZ

^{1}H NMR of CTP-PTZ was collected and depicted in **Figure. 2a**, which deduced the structure wherein six units of hydrazone Schiff base of PTZ linked to CTP ring core. The formation of imine group (-**H**C=N-NH-) was identified by a sharp singlet peak at 8.52 ppm for six protons of individual arms since the characteristic aldehyde proton peak at 9.78 ppm of R-PTZ-CHO was found to disappear. The six protons in hydrazone (-HC=N-N**H**-**P**) arms on CTP was corroborated significantly by broad singlet peak at 9.79 ppm and aromatic protons of PTZ appeared between 6.86-7.59 ppm while the aliphatic protons of octyl chain were noted in the range of 0.88-3.87 ppm. In particular, signal at 9.79 ppm for secondary amine proton of hydrazone (-HC=N-N**H**-**P**) tethered on phosphorus (V) centres of CTP was not effectively deshielded as similar to other type of hydrazone (-HC=N-N**H**-**CO**-), wherein adjacent electron deficient carbonyl group can effectively deshield to show a broad peak around 11.6-11.9 ppm.

^{13}C NMR spectrum of CTP-PTZ was recorded to further authenticate the structure (**Figure 2b)**. In particular, all ^{13}C nuclei correspond to the substrate, R-PTZ-CHO alone to be considered for the peak assignment in hybrid inorganic organic molecule, since the inorganic core substituted with six arms of hydrazide possess only phosphorus and nitrogen atoms. In **Figure 2b**, an intense ^{13}C NMR signal for the aldehyde group on PTZ unit was observed at 189.90 ppm, which experienced significant upfield shift to 160.76 ppm, while transformed to Schiff base of imine group by condensation. This upfield shift of 29.14 ppm was noted to be higher than the upfield shift of 20.26 ppm in our recent report on hydrazone Schiff base developed from hexakis (2-formylphenoxy) cyclotriphosphazene (HFP CTP) and salicylic hydrazide (SHyd) [37]. In detail, HFP CTP, six terminal aldehyde groups substituted in CTP ring found to exhibit upfield shift from 188.29 to 167.93 ppm while imine bond formed by condensation with SHyd [37].

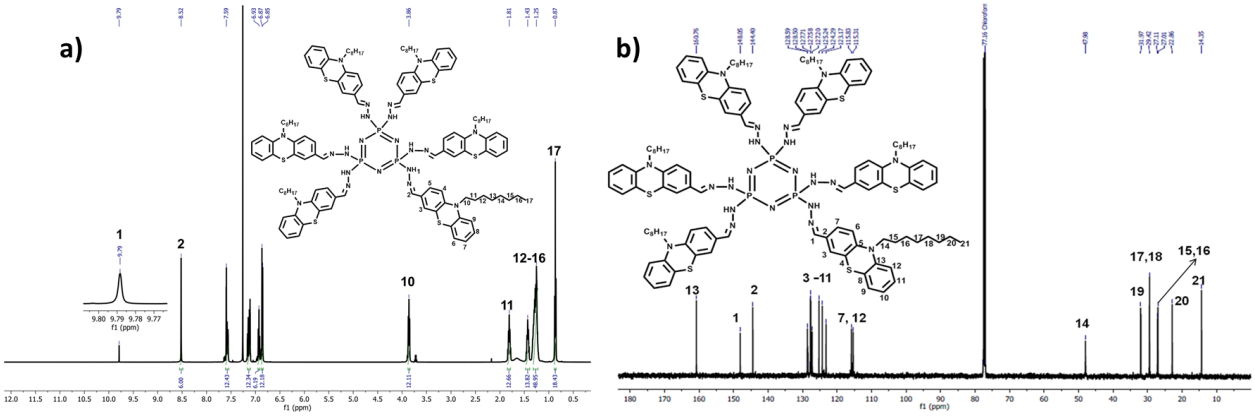

Figure 2. a) 1H NMR and b) 13C NMR data of hexakis hydrazone Schiff base of CTP, CTP-PTZ.

4. Photophysical studies

4.1 Steady state absorption data of precursor, key intermediates and hybrid molecule

A key aspect in developing novel multi-chromophoric assembly systems is that the final target molecule has to exhibit significant improvement in its photophysical properties such as tunable absorption, emission band and solvotochromism as compared to the individual starting components. In order to demonstrate this feature in the multicomponent assembly synthesised in the present work, we have carried out the steady state photophysical studies for the final target molecule as well as the precursor, phenothiazine. The steady state absorption properties of phenothiazine and the final inorganic-organic molecule, cyclotriphosphazene appended phenothiazine were performed in acetonitrile. The absorption spectrum of the final material CTP-PTZ was compared against the starting material, PTZ as well as the key intermediate compounds R-PTZ and R-PTZ-CHO as depicted in **Figure 3.** Pure phenothiazine showed a peak at 313 nm in acetonitrile. Based on the important aspect of processability, the final target molecule should be freely soluble in various solvents with differing polarities and to realise this goal we have attached a long linear alkyl chain to the rigid backbone which performs the role of solubilizing group.

The alkyl chain substituted phenothiazine did not show any significant variation in the absorption maximum (316 nm) due to the absence of any influence from the alkyl chain in phenothiazine electronic structure. However, when the formylation reaction on R-PTZ to obtain R-PTZ-CHO was conducted we observed a drastic variation in the absorption spectrum. The formylated product revealed two absorption bands, one relatively broad split band around 280-300 nm and another highly red shifted one at 386 nm. The higher energy (shorter wavelength band) was assigned to the localized aromatic $\pi-\pi^*$ transition of the phenothiazine ring and the lower energy (long wavelength) band is assigned to the charge transfer (CT) transition. The intensity of the CT transition absorption is lower than that of the $\pi-\pi^*$ transition. The observed charge transfer (CT) is from the donor phenothiazine unit to the acceptor aldehyde group. Finally, the absorption spectrum of the target molecule CTP-PTZ showed a further red shift towards the visible region (peak observed to exhibit λ_{max} at 411nm), a remarkable red shift of 25 nm towards the red. Covalent attachment of phenothiazine with cyclotriphosphazene through imine linkage provides a better electron accepting moiety for enhanced charge transfer process that shows pronounced red shift compared to phenothiazine. Certainly, the observed red shift in the synthesised inorganic-organic material into the visible region is promising. In this juncture, it is worth mentioning that the bare cyclotriphosphazene (used as core here in this study) showed λ_{max} at 175 nm. Two key findings from the above observations are as follows a) final molecule with long linear alkyl chain is soluble in various solvents in the wide relative polarity range of 0.099 (toluene) to 0.791 (methanol) with dielectric constant of the solvents varying from as low as 2.38 for toluene to as high as 36.7 for dimethylformamide b) the absorption spectrum can be tuned broadly when a multi-chromophoric approach is adopted.

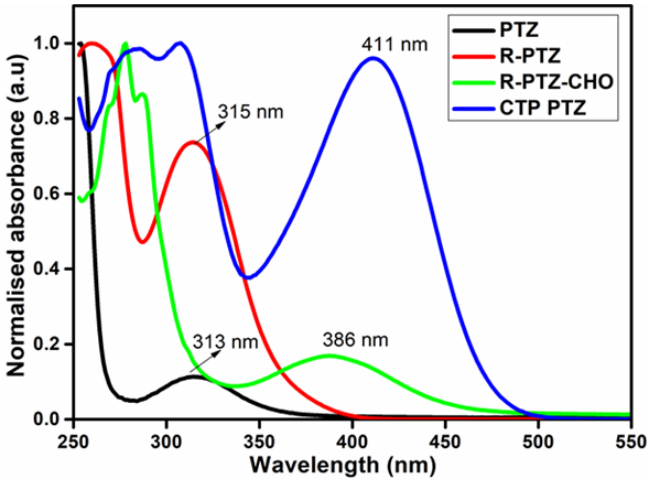

Figure 3. Comparison of UV-Vis data for the samples, PTZ, R-PTZ, R-PTZ-CHO and CTP-PTZ.

4.2 Effect of solvent on the photophysics

As the synthesised inorganic-organic hybrid material exhibits remarkable wide range solvent compatibility we performed steady state absorption, emission and time resolved photoluminescence measurements in various solvents. Dye solvation plays an important role in altering the spectroscopic properties of the optical materials especially in charge-transfer based dyes. Fascinating spectroscopic responses can be envisaged in the ground state or in the excited state due to the interactions that occurs between the solute and the solvent. As the synthesised molecule has not been reported earlier to the best of our knowledge and first of its kind, we intended to completely understand the photophysical behaviour of the compound and towards this task we have studied the molecule's behaviour in ten different solvents. These ten different solvents were categorised into three types (i) type A – apolar aprotic solvents (toluene, dichlromethane, chloroform and o-dichlorobenzene) (ii) type B – polar aprotic (acetonitrile, dimethylformamide and tetrahydrofuran) and finally (iii) type C – polar protic (methanol, iso-propanol and n-butanol). The absorption and emission properties of inorganic-organic hybrid, CTP-PTZ were measured in the above solvents and we have intentionally kept the concentration of the solutions low (1 x 10^{-5} M) in order to exclude any solute-solute interaction and self-absorption.

4.3 Steady state absorption studies in various solvents

Steady state UV-Vis absorption spectra of CTP-PTZ were also measured in various solvents at ambient temperature (25°C) as shown in **Figure 4**. The absorption profile of the compound was found to reveal two absorption bands, one around 300 nm and another one highly redshifted at around 410-420 nm depending on the solvent. In all the solvents under study, the molecule CTP-PTZ displayed relatively high molar extinction coefficient (~10^4 M^{-1} cm^{-1}). In all the solvents, the profile and shape of the absorption spectrum is not carried at all. A very slight red shift is observed in the absorption maxima of the CT state as we move from non-polar solvent like toluene (411 nm) to a polar solvent like n-butanol (416 nm). The observed weak positive solvatochromism indicates that the polar protic solvent environment causes small differences in dipole moments of the ground state of the synthesised inorganic-organic hybrid molecule.

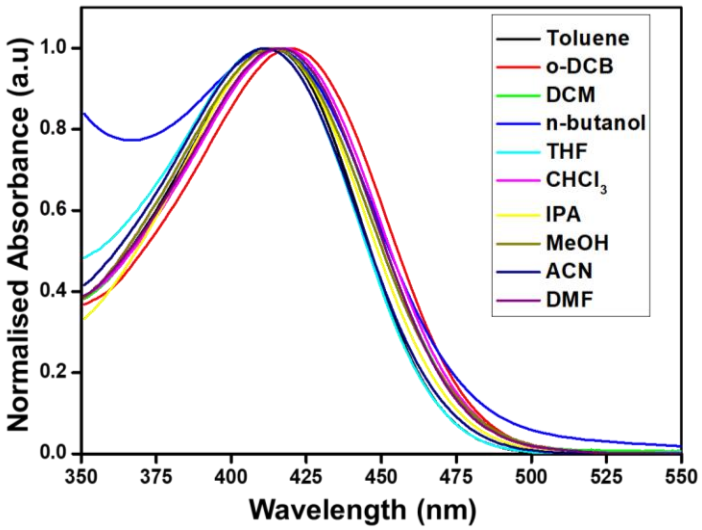

Figure 4. Comparison of normalized absorbance data (CT band) of CTP-PTZ measured in various solvents. Inset: Absorption spectra of CTP-PTZ in various solvents.

4.4. Steady state emission studies

After understanding the ground state properties, we moved on to decipher the excited state property of the synthesised inorganic-organic hybrid. We carried out the steady state photoluminescence study of the compound under investigation in the selected solvents. For the emission study, we excited the molecule at the respective absorption maximum (CT state) and monitored the emission. The normalised emission spectrum of the hybrid molecule in different solvents is shown in **Figure 5**. The photophysical properties like absorption maximum and the emission maximum values are listed in **Table 1** along with the dielectric constant and refractive index values of the solvents used in the study. The emission spectra of the hybrid molecule showed fascinating behaviour as compared to the absorption spectra. The observed emission spectra consisted of a relatively broad band with a maximum between 515 and 597 nm in all different solvents used in this investigation. With the increase in the solvent polarity we could clearly see a huge bathochromic shift in the observed emission maximum which confirms the charge transfer nature of the electronic transition. Interesting point to note here is that we have indeed noticed a pronounced effect of the solvent on the excited state of the molecule rather than in the ground state. This can be nicely correlated with the observed emission maximum in toluene the emission maximum was 515 nm and when we slightly increase the polarity of the solvent and move to solvents like chloroform and dichloromethane the emission maximum shifts to 541 nm and 555 nm respectively. Even larger bathochromic shift was observed when we move to polar aprotic solvents such as acetonitrile wherein the emission was observed at 583 nm. Further shifts towards longer wavelength were observed in polar protic solvent such as methanol (597 nm).

The observed large bathochromic shift in the emission maximum when we move from non-polar to polar solvent reveals that the excited state is stabilized in polar solvents or in other words the excited state dipole moment is larger than that of the ground state. This interaction causes the reduction of the excited state energy level, which causes enhancement in the rate of non-radiative decay. Previous reports with various other molecules also showed similar type of behaviour, that is the stabilisation of molecular excited state in polar medium which possesses lower energy levels and hence emitting at longer wavelength [40,41]. Further, two more salient features can be seen in the emission profile a) emission band full width at half maximum (FWHM) is increased with solvent polarity i.e. when we move from toluene to methanol and b) the synthesised CTP-PTZ show relatively strong emission in non-polar solvents than in polar protic solvents and this can be ascribed to the characteristic feature of a charge transfer state. We conclude this section by making the following points (i) tunable emission from yellow to green region depending on the solvent employed (ii) higher positive solvatofluorochromism with increasing solvent polarity that is ascertained with the observed bathochromic shift of 82 nm and (iii) self-quenching effect is minimised due to the greater separation of the excitation and emission wavelengths.

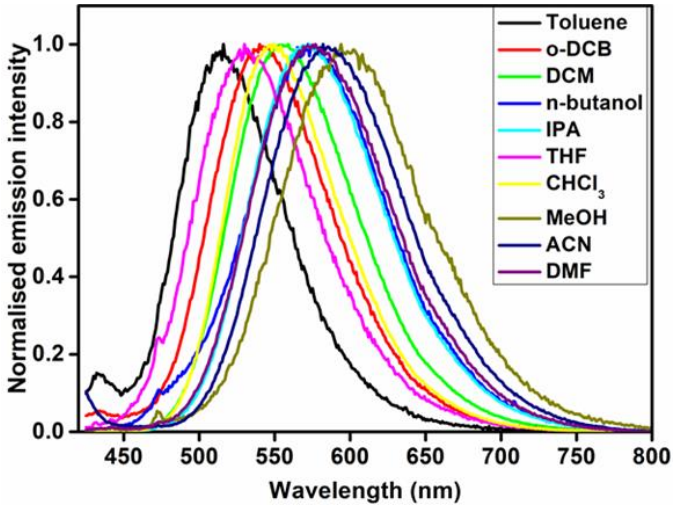

Figure 5. Steady state emission spectra of CTP-PTZ recorded in different solvents.

4.5. Solvent orientation polarizability and Stokes shift

As we have seen in the previous section the solvent molecule plays a crucial role in the observed spectroscopic properties. To gain further understanding on this phenomena we have attempted to correlate two factors a) solvent orientation polarizability (Δf) which accounts only for the spectral shifts due to the reorientation of the solvent molecules and depends on refractive index (n) and dielectric constant (ε) of the solvent [42,43] and b) stokes shift which can be defined as the difference between the wavelengths of emission and absorption maximum [44]. We first plotted the emission maximum of CTP-PTZ in each solvent against the dielectric constant of the respective solvent as this parameter generally describes polarity of the solvent. Reasonably moderate linear trend ($R^2 = 0.78$) was observed with reference to the emission peak maximum wherein the maximum shifts from 515 nm to 597 nm with increasing solvent dielectric constant and this clearly indicates that the solvent polarity has a pronounced effect on the excited state (**Figure 6**). The position of the emission maxima does not strictly correlate with the dielectric properties of the solvent, which is typical for the weak interactions between solvents and chromophores.

Table 1. Photophysical data of CTP-PTZ measured in various solvents.

Solvent	Refractive index	Dielectric constant	Relative polarity	Absorption maxima (λ_{abs}, nm)	υ_{abs} (cm^{-1})	Emission maxima (λ_{ems}, nm)	υ_{ems} (cm^{-1})	υ_{abs} (cm^{-1}) - υ_{ems} (cm^{-1})	Δf
Toluene	1.4961	2.38	0.099	413	24213	515	19417	4796	0.013
THF	1.4050	7.52	0.207	413	24213	529	18904	5309	0.210
$CHCl_3$	1.4459	4.81	0.259	420	23809	541	18484	5325	0.150
DCM	1.4244	8.93	0.309	419	23866	555	18018	5848	0.217
ODCB	1.5515	9.93	-	420	23810	539	18553	5257	0.186
DMF	1.4305	36.70	0.386	416	24038	574	17422	6616	0.274
ACN	1.3442	36.64	0.786	411	24331	583	17153	7178	0.305
IPA	1.3776	20.18	0.546	414	24155	572	17483	6672	0.277
BuOH	1.3988	17.50	0.586	415	24096	569	17575	6521	0.264
MeOH	1.3288	32.70	0.791	413	24213	597	16750	7463	0.308

After understanding the role of dielectric constant on the excited state, we moved on to calculate the stokes shift for CTP-PTZ in various solvents and the calculated value is tabulated in **Table 1**. The stokes shift values lie in the range of 4796–7463 cm^{-1}. As can be clearly decoded from the table, stokes shift values show significant increase with the increase in solvent polarity and this is attributed to the fact that the charge distribution is different in the excited state as compared to the ground state. Plot of the observed stokes shifts (Δv) against the solvent polarity parameter Δf (ε, n) usually called as Lippert-Mataga plot which accounts for general solvent effect was attempted [44, 45] (**Figure 6**). Estimation of the change in dipole moment of the excited state and ground state can be calculated from the magnitude of the slope. The expression for Δf (ε, n) is as follows

$$\Delta f\ (\varepsilon,) = [(\varepsilon - 1)/(2\varepsilon + 1)] - [(n^2 - 1)/(2n^2 + 1)]$$

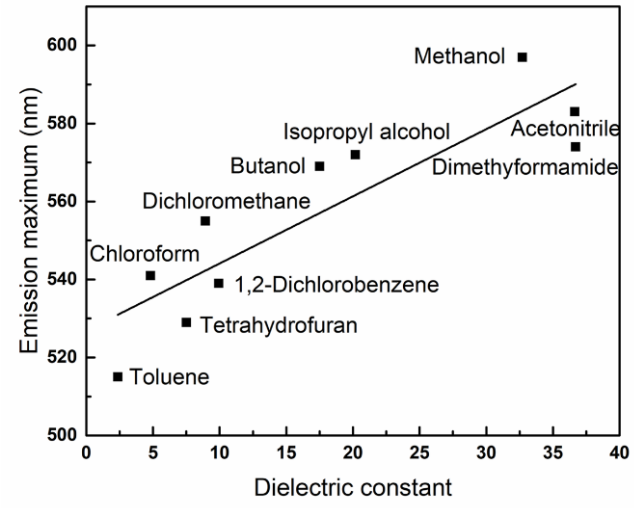

Figure 6. Plot of fluorescence emission maximum Vs dielectric constant of solvents.

As can be observed from **Figure 7a**, a poor-moderate linear correlation was noticed between the solvent polarity and magnitude of the stoke shift. Two pertinent observations are noted in this plot (i) when the Δf value becomes larger than 0.22, most of the data points fall on a straight line (ii) solvents with a polarity value smaller than 0.03 did not follow the trend and once this particular non-polar solvent (toluene) was removed the linear correlation fit becomes much better with R^2 values approaching 0.91(**Figure 7b**). These observations points to the fact that the stokes shift is not only affected by the polarity but other specific solvent effects like hydrogen bonding may also play a role [46].

This observation can be further substantiated from the region of polar solvents in the plot. Stokes shift observed for the hybrid molecule in methanol is somewhat higher than its value expected from the linear trend line shown in **Figure 7b** and this may be due to the result of the hydrogen bonding interaction between hydrazine NH of CTP-PTZ and the -OH group of methanol. Relative magnitudes of polarization and hydrogen bonding interactions are difficult to assess as methanol being both protic polar solvent and H-bonding in nature. Positive slope observed for CTP-PTZ in the plot reveals that the dipole moments of excited state increase with increasing polarity. To gain further insight on this, time resolved photoluminescence studies were carried out for CTP-PTZ in acetonitrile and methanol. These two solvents were chosen in such a way that they have comparable dielectric constant and one can form hydrogen bond (methanol) and the other

cannot (acetonitrile) with the solute. The fluorescence decay profiles were well fitted by applying a double-exponential function according to the equation $I(t) = A + B_1 \exp(-t/\tau_1) + B_2 \exp(-t/\tau_2)$ where B_1 and B_2 are pre exponential factors and τ_1 and τ_2 are respectively the fluorescence lifetimes. The χ^2 values were found to lie between 1.0-1.3 and the residuals are randomly distributed around zero. The observed fluorescence lifetime is in the nanosecond time scale. The CTP-PTZ hybrid molecule shows life times of 0.66 ns (79 %) and 2.66 ns (21%) with an average lifetime of 1.69 ns in acetonitrile whereas in methanol lifetimes of 0.55 ns (95%) and 4.64 ns (5%) with an average lifetime of 1.81 ns was observed. Moving from acetonitrile (polar aprotic) to methanol (polar protic) the fluorescence lifetime shows a marginal increase. The fluorescence lifetime of the molecule in these two different solvents also shows the influence of other solvent-solute interactions like hydrogen bonding interaction. Furthermore, in polar solvents the stabilization of charge separation decreases the radiative decay process [47]. Further studies to understand this effect in great detail are underway and will be reported elsewhere. Finally, we have also studied the photochemical stability of this new inorganic-organic luminescent hybrid material as this parameter plays a key role for any potential application. 10 mL of the as-synthesised CTP-PTZ dissolved in methanol was transferred into quartz glass containers and irradiated with continuous-wave UV light (365 nm) at specified intensity at ambient temperature. Absorption spectrum of the solution was measured before and after UV irradiation for 150 minutes (interval 15 minutes) and we could not see any apparent photobleaching of the compound as no appreciable change was noted either in the absorbance or in the profile of the absorption spectrum.

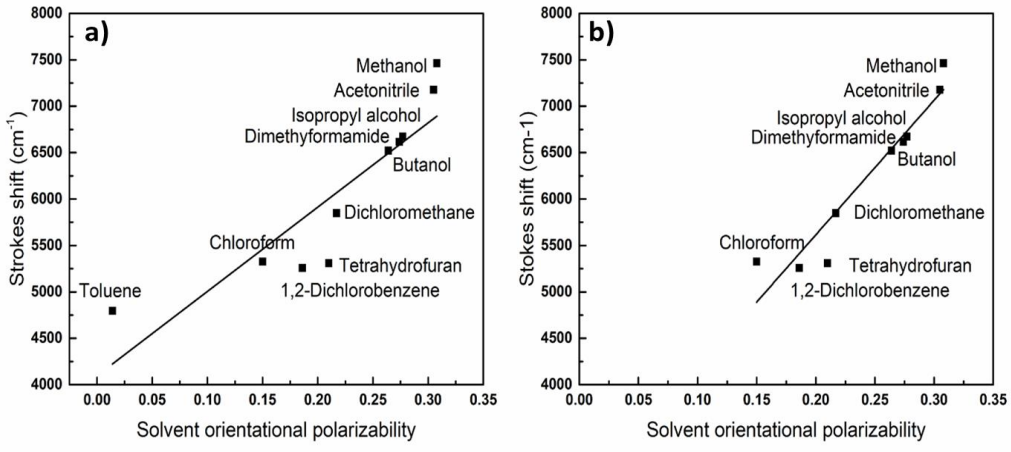

Figure 7. (a) Lippert-Mataga plot for the determined values of stokes shift in wavenumbers against solvent orientation polarizability, Δf(ε, n) (b) Lippert-Mataga plot for the determined values of stokes shift in wavenumbers against solvent orientation polarizability, Δf(ε, n) (toluene excluded)

5. Cyclic voltammetry studies

5.1 Cyclic voltammetry of precursors and hybrid molecule

The detailed photophysical studies accounted in the last section motivated us to understand the energy levels of the as synthesised organic-inorganic hybrid material. To deduce this parameter, cyclic voltammetry (CV) studies were carried out to determine the highest occupied molecular orbital (HOMO) levels of the molecule as the onset oxidation potential corresponds to the energy of the HOMO and from the HOMO levels and $E_{0\text{-}0}$ value we can determine the LUMO levels. Cyclic voltammogram of the compound recorded in acetonitrile under nitrogen atmosphere is shown in **Figure 8**. The E_{HOMO} value obtained from the oxidation onset potential (Fc/Fc^+ as an internal standard) is found to be -4.93 eV. We have calculated the LUMO level, E_{LUMO} using the equation $E_{LUMO} = E_{HOMO} - E_{0-0}$. The 0-0 transition energy was estimated from the intersection points of the normalized absorption and emission spectra. The calculated E_{LUMO} value was found to be – 2.25 eV and any entropy change during light excitation was not considered. The energy level values of this material show that this material can be employed as a charge transport material in inorganic-organic hybrid perovskite solar cells and further work in this direction is under progress.

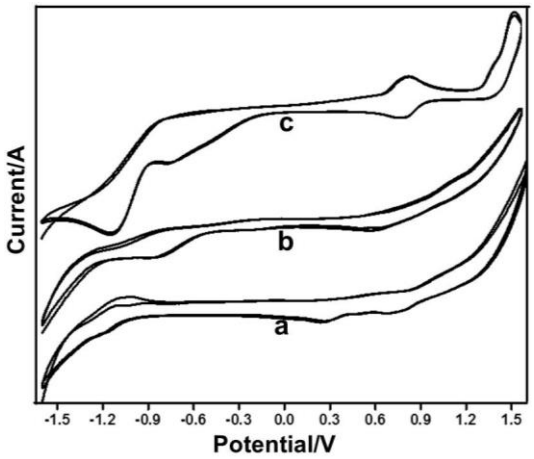

Figure 8. CV data of precursors, a) PTZ, b) CTP and c) redox behaviour of CTP-PTZ.

5.2. Variation of scan rate

The cyclic voltammograms were recorded in acetonitrile medium (nitrogen atmosphere) in the presence of supporting electrolyte, tetrabutylammonium hexafluorophosphate (Bu_4NPF_6) solution (0.1 **M**) at different scan rates 10, 25, 50, 75 and 100 mV/s. The cyclic voltammograms display well defined cathodic and anodic peaks (**Figure 9a**). Quasi-reversible one-electron transfer redox process of CTP-PTZ was observed. Cyclic voltammogram of pristine CTP and PTZ recorded under identical condition did not reveal any well-defined redox peaks (**Figure 8**). This observation clearly reveals that the uniform assembly of PTZ unit on the periphery of CTP via Schiff base motifs by condensation has indeed had a profound effect on the redox properties. Cyclic voltammogram recorded at variable scan rates (10, 25, 50, 75 and 100 mV/s) show that the peak current intensity proportionally increases with respect to the increase in scan rate and the redox potential values were noted to exhibit minor variation with variable scan rate. Moreover, the peak shape of all CV data was identified to show single type of redox process consistently at all scan rates. The single redox potential revealed that all six different PTZ units on CTP ring were determined to undergo redox process concurrently and such analogous redox behaviour was reported by us earlier on a multi-ferrocene assembly on CTP [34]. Electrochemically quasi-reversible behaviour and chemically reversible behaviour was seen with respect to the trend in the redox potential values of CTP-PTZ and the ratio of anodic and cathodic current value (Ip_a/Ip_c=1) respectively.

To further understand the electrochemical process occurring at the electrode interface we plotted the variation of the current intensity (both anodic and cathodic) against the square root of scan rate ranging from 10 to 100 mVs^{-1}. In **Figure 9b**, an excellent least squares correlation for oxidation (R^2=0.997) and reduction (R^2=0.977) process was obtained.

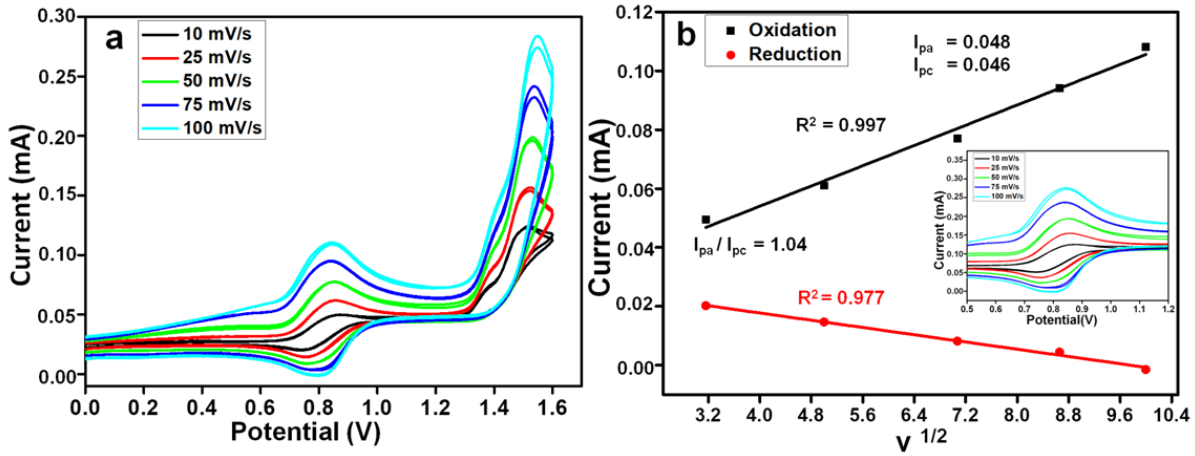

Figure 9. CV data of a) CTP-PTZ recorded at different scan rate and b) linear correlation plot for the square root of anodic and cathodic current versus scan rate.

6. Thermal stability studies

As the synthesised inorganic-organic hybrid molecule exhibits good spectral features with promising photostability we intended to investigate its thermal stability as well. The onset degradation temperature (T_d) is usually employed as an essential parameter to decipher the thermal stability. Thermal gravimetric analysis (TGA) data was collected under nitrogen atmosphere from ambient temperature to 1000 °C to determine the thermal stability of samples to be studied such as R-PTZ-CHO, CTP-Hyd and CTP-PTZ (**Figure 10**). The 5 % weight loss temperature (T_d) parameter is used to analyse the thermal stability and the T_d values of R-PTZ-CHO, CTP-Hyd and CTP-PTZ was found to be 153°C, 280°C and 326°C respectively. The data for the hybrid sample, CTP-PTZ revealed the enhancement in thermal stability due to the existence of flame-retardant P-N framework [48-50].

The initial mass loss around 100 °C is attributed to the vaporization of moisture from the samples under analysis. TGA profile with multiple steps of degradation in the graph represented the decomposition of existing functional groups and backbone of the structure. The pure organic composition of PTZ-CHO was found to undergo facile decomposition with minimum residual mass (3.1 %). In case of CTP-Hyd, the maximum quantity of residual mass (37.6 %) was noticed due to the major quantity of P-N framework containing hydrazide arms with respect to inorganic structure. As a hybrid sample, CTP-PTZ revealed the enhancement in thermal stability properties with high value of T_d (326 °C) and the considerable quantity of residual mass (34.8 %) due to the existence of P-N heterocycle.

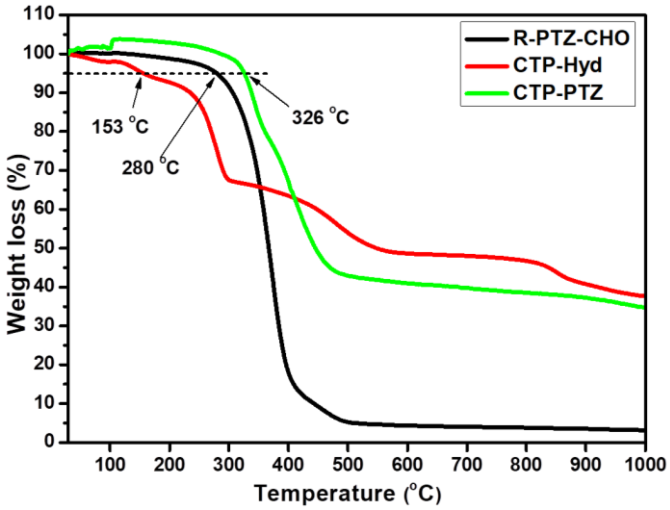

Figure 10. Thermograms of samples, a) PTZ-CHO, b) CTP-Hyd and c) CTP-PTZ.

7. Conclusions

For the first time, the synthesis of the inorganic organic luminous hybrid molecule CTP-PTZ, which consists of six PTZ hydrazone Schiff bases assembled on the periphery of an inorganic heterocycle known cyclotriphosphazene, has been reported. The structure of the synthesised molecule was unequivocally validated by FT-IR, multi-nuclear NMR, including ^{1}H, and ^{13}C NMR data. Interesting photophysical, electrochemical, and thermal properties were found as a result of the multi-component assembly of organic chromophores on the stable inorganic core. Particularly, increased positive solvatochromism with increasing solvent polarity and tunable emission from the yellow to green area were observed. Due to the presence of the flame-retardant P-N framework, the hybrid CTP-PTZ demonstrate good thermal stability as indicated by the high Td value of 326 °C.

REFERENCES:

[1] Lebeau, B. and Innocenzi, P., Hybrid materials for optics and photonics. *Chemical Society Reviews*, 2011, *40*, 886-906.

[2] Astruc, D., Boisselier, E. and Ornelas, C., Dendrimers designed for functions: from physical, photophysical, and supramolecular properties to applications in sensing, catalysis, molecular electronics, photonics, and nanomedicine. *Chemical reviews*, *110*, 1857-1959.

[3] Ashford, D.L., Gish, M.K., Vannucci, A.K., Brennaman, M.K., Templeton, J.L., Papanikolas, J.M. and Meyer, T.J., 2015. Molecular chromophore–catalyst assemblies for solar fuel applications. *Chemical Reviews*, *115*(23), pp.13006-13049.

[4] Wang, J.C., Hill, S.P., Dilbeck, T., Ogunsolu, O.O., Banerjee, T. and Hanson, K., Multimolecular assemblies on high surface area metal oxides and their role in interfacial energy and electron transfer. *Chemical Society Reviews*, 2018, *47*, 104-148.

[5] Brauge, L., Veriot, G., Franc, G., Deloncle, R., Caminade, A.M. and Majoral, J.P., 2006. Synthesis of phosphorus dendrimers bearing chromophoric end groups: toward organic blue light-emitting diodes. *Tetrahedron*, *62*(51), pp.11891-11899.

[6] Chetan, B., and Chain-Shu, H., Organic Nanoparticles and Organic-Inorganic Hybrid Nanocomposites: Synthesis and Photophysical Characterization, Lambert Academic Publishing, 2011.

[7] Mahmud, A., Khan, A.A., Islam, S., Voss, P. and Ban, D., Integration of organic/inorganic nanostructured materials in a hybrid nanogenerator enables efficacious energy harvesting via mutual performance enhancement. *Nano Energy*, 2019, *58*, 112-120.

[8] Sanchez, C., Belleville, P., Popall, M. and Nicole, L., Applications of advanced hybrid organic–inorganic nanomaterials: from laboratory to market. *Chemical Society Reviews*, *40*, 2011, 696-753.

[9] Hassan, Z., Matt, Y., Begum, S., Tsotsalas, M. and Bräse, S., Assembly of Molecular Building Blocks into Integrated Complex Functional Molecular Systems: Structuring Matter Made to Order. *Advanced Functional Materials*, 2020, p.1907625.

[10] Lees, A. J. ed., *Photophysics of organometallics* 2010, Vol. 29, Springer Science & Business Media.

[11] Wei, Y., Laurent, R., Majoral, J.P. and Caminade, A.M., Synthesis and characterization of phosphorus-containing dendrimers bearing rhodamine derivatives as terminal groups. *Arkivoc*, 2010, *10*, 318-327.

[12] Qiu, J., Hameau, A., Shi, X., Mignani, S., Majoral, J.P. and Caminade, A.M., Fluorescent Phosphorus Dendrimers: Towards Material and Biological Applications. *ChemPlusChem*, 2019, *84*, 1070-1080.

[13] 20. Xue, P., Yao, B., Liu, X., Sun, J., Gong, P., Zhang, Z., Qian, C., Zhang, Y. and Lu, R., Reversible mechanochromic luminescence of phenothiazine-based 10, 10′-bianthracene derivatives with different lengths of alkyl chains. *Journal of Materials Chemistry C*, 2015, *3*, 1018-1025.

[14] Brauge, L., Caminade, A.M., Majoral, J.P., Slomkowski, S. and Wolszczak, M., Segmental mobility in phosphorus-containing dendrimers, Studies by fluorescent spectroscopy. *Macromolecules*, 2001, *34*, 5599-5606.

[15] Jia, J. and Wu, Y., Alkyl length dependent reversible mechanofluorochromism of phenothiazine derivatives functionalized with formyl group. *Dyes and Pigments*, 2017, *147*, 537-543.

[16] Sachdeva, T., Bishnoi, S. and Milton, M.D., Multi-Stimuli Response Displaying Novel Phenothiazine-Based Non-Planar D-π-A Hydrazones: Synthesis, Characterization, Photophysical and Thermal studies. 2017, *ChemistrySelect*, *2*, 11307-11313.

[17] Gai, F., Li, X., Zhou, T., Zhao, X., Lu, D., Liu, Y. and Huo, Q., Silica cross-linked nanoparticles encapsulating a phenothiazine-derived Schiff base for selective detection of Fe (III) in aqueous media. *Journal of Materials Chemistry B*, 2014, *2*, 6306-6312.

[18] Chandrasekhar, V., Azhakar, R., Murugesapandian, B., Senapati, T., Bag, P., Pandey, M.D., Maurya, S.K. and Goswami, D., Synthesis, Structure, and Two-Photon Absorption Studies of a Phosphorus-Based Tris Hydrazone Ligand (S) P [N (Me) N-CH-C_6H_3-2-OH-4-N $(CH_2CH_3)_2]_3$ and Its Metal Complexes. *Inorganic chemistry*, 2010, *49*, 4008-4016.

[19] Chandrasekhar, V. and Thomas, K.J., Coordination and organometallic chemistry of cyclophosphazenes and polyphosphazenes. *Applied organometallic chemistry*, 1993, *7*, 1-31.

[20] Chandrasekhar, V. and Nagendran, S., Phosphazenes as scaffolds for the construction of multi-site coordination ligands. *Chemical Society Reviews*, 2001, *30*, 193-203.

[21] V. Chandrasekhar, *Inorganic and Organometallic Polymers*, Springer-Verlag, 2005.

[22] Mukundam, V., Dhanunjayarao, K., Mamidala, R. and Venkatasubbaiah, K., Synthesis, characterization and aggregation induced enhanced emission properties of tetraaryl pyrazole decorated cyclophosphazenes. *Journal of Materials Chemistry C*, 2016, *4*, 3523-3530.

[23] İbişoğlu, H., Kılıç, Z., Yuksel, F. and Tümay, S.O., 2020. Synthesis, characterization, photophysical and intramolecular energy transfer properties of oxy-naphthylchalcone appended cyclotriphosphazene cores. *Journal of Luminescence*, *222*, p.117125.

[24] Rao, M.R., Bolligarla, R., Butcher, R.J. and Ravikanth, M., Hexa boron-dipyrromethene cyclotriphosphazenes: synthesis, crystal structure, and photophysical properties. *Inorganic chemistry*, 2010, *49*, 10606-10616.

[25] Nair, V.S., Pareek, Y., Karunakaran, V., Ravikanth, M. and Ajayaghosh, A., Cyclotriphosphazene appended porphyrins and fulleropyrrolidine complexes as supramolecular multiple photosynthetic reaction centers: Steady and excited states photophysical investigation. *Physical Chemistry Chemical Physics*, 2014, *16*, 10149-10156.

[26] Ün, İ., İbişoğlu, H., Ün, Ş.Ş., Çoşut, B. and Kılıç, A., Syntheses, characterizations, thermal and photophysical properties of cyclophosphazenes containing adamantane units. *Inorganica Chimica Acta*, 2013, *399*, 219-226.

[27] Uslu, A., Tümay, S.O., Şenocak, A., Yuksel, F., Özcan, E. and Yeşilot, S., Imidazole/benzimidazole-modified cyclotriphosphazenes as highly selective fluorescent probes for Cu^{2+}: synthesis, configurational isomers, and crystal structures. *Dalton Transactions*, 2017, *46*, 9140-9156.

[28] Özcan, E., Tümay, S.O., Alidağı, H.A., Çoşut, B. and Yeşilot, S., A new cyclotriphosphazene appended phenanthroline derivative as a highly selective and sensitive OFF–ON fluorescent chemosensor for Al^{3+} ions. *Dyes and Pigments*, 2016, *132*, 230-236.

[29] Haddon, R.C., Mayo, S.L., Chichester, S.V. and Marshall, J.H., Phenalene-phosphazene complexes: injection of electron spin density into the cyclotriphosphazene ring system. *Journal of the American Chemical Society*, 1985, *107*, 7585-7591.

[30] Haddon, R.C., Chichester-Hicks, S.V. and Mayo, S.L., Phenalene-phosphazene complexes: effect of exocyclic charge densities on the cyclotriphosphazene ring system. *Inorganic Chemistry*, 1988, *27*, 1911-1915.

[31] Çiftçi, G.Y., Şenkuytu, E., Durmuş, M., Yuksel, F. and Kılıç, A., Structural and fluorescence properties of 2-naphthylamine substituted cyclotriphosphazenes. *Inorganica Chimica Acta*, 2014, *423*, 489-495.

[32] Majoral, J.P. and Caminade, A.M., 2019. Phosphorhydrazones as Useful Building Blocks for Special Architectures: Macrocycles and Dendrimers. *European Journal of Inorganic Chemistry*, *2019*(11-12), pp.1457-1475.

[33] Galliot, C., Caminade, A.M., Dahan, F. and Majoral, J.P., Synthesis, Structure, and Reactivity of Stable PN Heterocycles with Two and Six Methyleneamine Units: $[H_2C{=}N{=}N(Me)]_2P(S)(Ph)$ and $[H_2C{=}N{=}N(Me)]_6P_3N_3$. *Angewandte Chemie International Edition*, 1993, *32*, 1477-1479.

[34] Chandrasekhar, V., Senthil A. Gurusamy Thangavelu, Nagendran, S., Krishnan, V., Azhakar, R., Butcher, R. J. Cyclophosphanzene hydrazides as scaffolds for multi-ferrocenyl assemblies: Synthesis, structures and electrochemistry *Organometallics*, 2003, *22*, 976 –986

[35] Chandrasekhar, V., Senthil A. Gurusamy Thangavelu, Azhakar, R., Pandian, B. M. Cyclophosphazene-supported tetranuclear copper assembly containing fifteen contiguous inorganic rings. *Inorg. Chem.* 2008, *47*, 1922-1924

[36] Chandrasekhar, V., Senthil A. Gurusamy Thangavelu, Azhakar, R., Pandian, M. 36- and 42- Membered cyclophosphazene-containing macrocycles *Tetrahedron Lett.*, 2006, *47*, 8365-8368.

[37] Dinesh Kumar, C., Ananthan Alagumalai, Joydev Acharya, Pawan Kumar, Koustav Sarkar, Senthil A. Gurusamy Thangavelu, Vadapalli Chandrasekhar. "Functionalized Iron Oxide Nanoparticles Conjugate of Multi-Anchored Schiff's Base Inorganic Heterocyclic Pendant Groups: Cytotoxicity Studies." *Applied Surface Science*, 2020, *501*, 143963.

[38] Çiftçi, G.Y., Şenkuytu, E., Durmuş, M., Yuksel, F. and Kılıç, A. Structural and fluorescence properties of 2-naphthylamine substituted cyclotriphosphazenes. Inorganica Chimica Acta, ., 2014, 423, pp.489-495.

[39] Majoral, J.P. and Caminade, A.M. Phosphorhydrazones as useful building blocks for special architectures: macrocycles and dendrimers. European Journal of Inorganic Chemistry, 2019 (11-12), pp.1457-1475.

[40] Galliot, C., Caminade, A.M., Dahan, F. and Majoral, J.P. Synthesis, Structure, and Reactivity of Stable PN Heterocycles with Two and Six Methyleneamine Units:$[H_2C{=}N{-}N(Me)]_2$ P (S)(Ph) and $[H_2C{=}N{-}N(Me)]_6P_3N_3$. Angewandte Chemie International Edition in English, 1993, 32(10), pp.1477-1479.

[41] Chandrasekhar, V., Senthil Andavan, G.T., Nagendran, S., Krishnan, V., Azhakar, R. and Butcher, R.J.. Cyclophosphazene hydrazides as scaffolds for multi-ferrocenyl assemblies: synthesis, structure, and electrochemistry. Organometallics, 2003, 22(5), pp.976-986.

[42] Chandrasekhar, V., Andavan, G.T.S., Azhakar, R. and Pandian, B.M. Cyclophosphazene-supported tetranuclear copper assembly containing 15 contiguous inorganic rings. Inorganic chemistry, 2008, 47(6), pp.1922-1924.

[43] Chandrasekhar, V., Andavan, G.T.S., Azhakar, R. and Pandian, B.M. 36-and 42-Membered cyclophosphazene-containing macrocycles. Tetrahedron letters, 2006, 47(47), pp.8365-8368.

[44] Xie, Z., Midya, A., Loh, K.P., Adams, S., Blackwood, D.J., Wang, J., Zhang, X. and Chen, Z., Highly efficient dye-sensitized solar cells using phenothiazine derivative organic dyes. Progress in Photovoltaics: Research and Applications, 2010, 18(8), pp.573-581.

[45] Allcock, H.R. Recent advances in phosphazene (phosphonitrilic) chemistry. chemical Reviews, 1972, 72(4), pp.315-356.

[46] Dey, J. and Warner, I.M. Charge-transfer effects on the fluorescence spectra of 9-aminocamptothecin steady-state and time-resolved fluorescence studies. Journal of Photochemistry and Photobiology A: Chemistry, 1998, 116(1), pp.27-37.

[47] Vázquez, M.E., Blanco, J.B. and Imperiali, B. Photophysics and biological applications of the environment-sensitive fluorophore 6-N, N-dimethylamino-2, 3-naphthalimide. Journal of the American Chemical Society, 2005, 127(4), pp.1300-1306.

[48] Lakowicz, J.R. ed.. Principles of fluorescence spectroscopy. Boston, MA: springer US 2006.

[49] Srividya, N., Ramamurthy, P. and Ramakrishnan, V.T. Solvent effects on the absorption and fluorescence spectra of some acridinedione dyes: determination of ground and excited state dipole moments. Spectrochimica Acta Part A: Molecular and Biomolecular Spectroscopy, 1997, 53(11), pp.1743-1753.

[50] Chelike, D.K., Alagumalai, A., Muthukumar, V.R., Thangavelu, S.A.G. and Krishnamoorthy, A.,. Tunable yellow–green emitting cyclotriphosphazene appended phenothiazine hydrazone hybrid material: Synthesis, characterisation, photophysical and electrochemical studies. New Journal of Chemistry, 2020, 44(31), pp.13401-13414.